The effect of rolling friction on vibro-impact damped boring bars

Arjun Patel
Department of Mechanical Engineering
Indian Institute of Technology Kanpur
Kanpur, India
aspatel@iitk.ac.in

Mohit Law
Department of Mechanical Engineering
Indian Institute of Technology Kanpur
Kanpur, India
mlaw@iitk.ac.in

Pankaj Wahi
Department of Mechanical Engineering
Indian Institute of Technology Kanpur
Kanpur, India
wahi@iitk.ac.in

***Abstract*— Machining vibrations in an impact-damped boring bar are suppressed through momentum transfer from the bar to a freely moving mass. The effectiveness of this mechanism, however, depends on the ability of the mass to overcome frictional resistance while rolling within the bar cavity. This paper explicitly includes rolling friction in a model-based analysis to evaluate the damping potential of a ball-type impact damper. The bar is represented by a lumped-parameter model with parameters derived from Euler–Bernoulli beam theory, and rolling friction at the ball–bar interface is described using a dry-friction model. Our analysis shows that vibro-impact dynamics and damping potential are strongly influenced by the forcing frequency, gap, and rolling friction. The inclusion of friction enables impacts even at larger gap sizes but yields lower damping than the frictionless model. Although experimental validation is still required, the results show that neglecting friction can overestimate damping performance and lead to an inaccurate prediction of the optimal gap for a given excitation.**

Keywords—Boring bar, Rolling friction, Vibro-impact, Impact damper, Passive damping

I. Introduction

Cutting forces excite the boring bar, inducing oscillatory motion. These process-induced vibrations degrade surface finish and dimensional accuracy, and if not properly controlled or damped, they can even cause damage to the tool and workpiece. This paper proposes a vibro-impact damping solution for vibration-free boring. A vibro-impact system typically consists of an oscillating free mass that intermittently collides with constraints or another structure, with the primary objective of suppressing its vibrations [1]. Depending on the nature of these impacts, they may either suppress vibrations or destabilize the bar, emphasizing the need for a thorough model-based parametric analysis to identify the optimal design and material properties of the vibro-impact system.

Although such passive dampers have been studied both theoretically [2]–[8] and experimentally [7]–[12] over time and are regarded as proven damping solutions, their application in cutting tools remains limited. Among these reports, the work of Thomas et al. [7] stands out as a foundational contribution, providing the first experimental evidence of the effective performance of impact dampers in boring bars, along with their model-based verification. Although their experiments demonstrated the high effectiveness of the impact damper, the design and analysis were based on an impacting mass supported by soft springs rather than a freely moving mass. Since the impacting mass in their system behaves like an oscillator, it can potentially act as a tuned or detuned vibration absorber. Such hybrid damping concepts require additional parameters to be tuned for optimal performance, thereby reducing the robustness of vibro-impact systems. A similar hybrid concept was also investigated in a recent study [6].

The mathematical model reported in [7] employed a single-degree-of-freedom (SDOF) lumped-parameter representation of the boring bar with a spring-supported impacting mass, with energy dissipation from collisions modeled using impulsive forces. In contrast, the present work builds upon that model but considers an unconstrained, freely moving mass. Another approach to modeling energy dissipation through impacts is to assume a spring–dashpot mechanism [4], [5], [13] between the free mass and the main system during impact. However, the spring stiffness and damping coefficients are generally unknown and must be estimated using impact mechanics models [14]. Since modeling the contact as a viscoelastic spring–dashpot system involves nonlinear force–deformation relationships and uncertain parameters, we adopt a simpler approach. Instead of applying impulsive forcing as in [7] or using a viscoelastic contact model, the velocities of the boring bar and damper mass are updated after each impact using linear momentum balance and the coefficient of restitution (COR) as reported in [1].

Prior model-based studies [2], [5]–[8] neglected the friction at the interface between the free mass and its enclosure. Since ignoring the friction effect can underestimate the coupled system's dynamics, the present work incorporates rolling friction between the free mass and the enclosure's bottom surface in the boring bar, using the model reported in [15]. Although a simplified lumped-parameter model inspired by previous studies [6]–[8] is used here to represent the boring bar's dynamics, the inclusion of rolling friction represents a key novel aspect of this work. In addition, the systematic evaluation of damping performance near resonance under harmonic forcing across varying gap sizes constitutes the novel contribution of this study.

The remainder of the paper is organised as follows. Section II of the paper presents the mathematical model of the combined boring bar and damper system and the governing equations, along with the method of solution. Section III of the paper discusses the numerical results of model-based analysis and provides the details of the damping potential of the vibro-impact system. Finally, the main conclusions of this current study are summarized in Section IV.

II. Mathematical model of the Combined system

This section begins by discussing the possible design and mathematical model of the combined boring bar and vibro-impact system, followed by the governing equations and the solution methodology.

A. Design and model of an impact-damped boring bar

A simple construction of the boring bar is shown in Fig. 1(a), featuring a cavity drilled across its diameter at an appropriate distance from the free end to house a free mass. In this study, the free mass is a spherical ball placed within the cavity, enclosed by two side plugs to retain it during machining. The boring bar has a cartridge at the free end to hold the cutting insert, which is connected to the main bar via an end plug, while the opposite end is fixed in the clamping holder. The cavity is designed with a clearance between the ball and the side plugs, allowing the vibrating bar to excite the ball and induce impacts. Although the gap size is an important design parameter, the damping performance also depends on other factors, including the mass and material of the free ball, the coefficient of restitution, and the location of the cavity. By carefully selecting a combination of these parameters, the impacts can effectively suppress vibrations, resulting in improved surface finish and enhanced machining performance.

The boring bar, including the side plugs, is assumed to be made entirely of steel, with length L and diameter D. For the forced vibration analysis, a length-to-diameter ratio of approximately 7 is considered, corresponding to a diameter of 25 mm and a length of 175 mm. Since the first bending mode of vibration is the critical mode, the boring bar can be approximated as a simple SDOF system, for which a lumped-parameter model provides a reasonable approximation. The mechanical model of the combined system used in this study is shown in Fig. 1(b), which represents the reduced SDOF model where the mass, stiffness, and damping of the hollow bar are assumed to be lumped and denoted by M, K, and C, respectively. These parameters are evaluated using standard Euler–Bernoulli beam theory [16]. The internal damping of the bar is estimated by assuming a damping ratio of 0.01 for the steel.

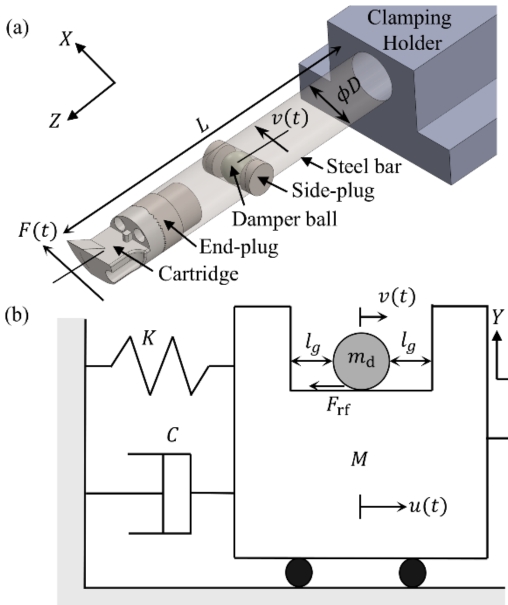

Fig. 1: (a) Schematic of a boring bar integrated with an impact damper, and (b) Mechanical model showing SDOF system of boring bar with a damper ball.

The spherical ball of mass m_d is placed inside the cavity at its midpoint, leaving equal gaps of l_g on both sides. The bar is excited by the cutting force $F(t)$ acting at the cutting (free) end, resulting in oscillatory motion with an amplitude of $u(t)$. This vibratory motion of the bar excites the ball, leading to repeated collisions. Mathematically, an impact occurs when $v(t) - u(t) = \pm l_g$, where $v(t)$ is the displacement of the ball and l_g is half the total gap. In other words, an impact takes place whenever the relative displacement between the ball and the bar equals the available gap on either side. Since the ball rolls over the cavity surface, a rolling friction force, denoted as F_rf, is considered to represent the resistance at the interface that must be overcome to initiate and sustain motion. The governing equations are presented next.

B. Governing equations of the combined system

The governing equations for the coupled boring bar–impact damper system are given as follows:

$$M\ddot{u} + C\dot{u} + Ku = F - F_\mathrm{rf} \tag{1}$$

$$m_\mathrm{d}\ddot{v} = F_\mathrm{rf} \tag{2}$$

wherein F_rf in Eqs. (1–2) is expressed as follows:

$$F_\mathrm{rf} = \frac{1}{r}\eta_\mathrm{rf} m_\mathrm{d} \mathrm{g}\big(\mathrm{sgn}(\dot{w})\big);$$
$$\mathrm{sgn}(\dot{w}) = \begin{cases} 1, & \dot{w} > 0; \\ 0, & \dot{w} = 0; \\ -1, & \dot{w} < 0, \end{cases} \tag{3}$$

wherein r is the radius of the ball, η_rf is the coefficient of rolling friction, and g is the acceleration constant due to gravity. $\dot{w}$ is the relative velocity, and w is the relative displacement defined as $w = v(t) - u(t)$. The rolling friction model used here is approximated as a dry (Coulomb) friction formulation [15] to account for micro-slip and hysteric losses as the ball rolls on the cavity. In this study, the cutting forces are approximated as a periodic sinusoidal excitation of the form $F = F_o \sin \Omega t$, wherein F_o is the magnitude of external forcing, and Ω is the excitation frequency used in the dynamic analysis. The next subsection describes the solution method.

C. Numerical solution of the combined system

The dynamics of an impact-damped boring bar is analyzed by solving Eqs. (1-2) numerically using the fourth-order Runge–Kutta method. The system is initialized at $t = 0$ with both the bar and the ball at rest, and the ball positioned at the center of the cavity. A uniform time step of 10^{-6} seconds is used to integrate Eqs. (1-2) with the aid of Eq. (3). At each time step, the impact condition, $w = \pm l_g$ is checked. If the condition is met, the post-impact velocities of both the bar and the ball are updated. The post-impact velocities are determined using the conservation of linear momentum in conjunction with the COR. The final expressions for the bar's velocity and the relative velocity after impact are given as follows:

$$\dot{u}_+ = \dot{u}_- + \frac{\mu(1+e)}{(1+\mu)}\dot{w}_-; \tag{4}$$

$$\dot{w}_+ = -e\dot{w}_-, \tag{5}$$

wherein μ is the mass ratio defined as m_d/M, and e denotes COR. The subscripts '$-$' and '$+$' denote the instants immediately before and after the impacts, respectively. After each impact, the post-impact velocities are evaluated using Eqs. (4-5), and the complete displacement and velocity histories of both the bar and the ball are computed.

III. RESULTS AND DISCUSSION

This section presents a model-based investigation of the damping potential of a vibro-impact system integrated with a boring bar. The force magnitude F_o is set to 15 N, representing the oscillatory component of cutting forces observed during aluminum machining at a feed of 0.1 mm/rev and depths of cut between 0.1 mm and 0.2 mm. The steady (DC) component of the cutting force is not considered in the analysis. To evaluate the damping performance, the forced excitation frequency is swept around the resonance while maintaining a constant force magnitude. The frequency ratio, defined as the forcing frequency divided by the system's natural frequency, is varied from 0.95 to 1.05 in increments of 0.01. The bar's material properties are specified as Young's modulus $E = 200$ GPa, and mass density $\rho = 7850$ kg/m^3, representing the properties of steel. A cavity of 15.1 mm length and 17 mm diameter is designed to house a 15 mm diameter damper ball, providing a total clearance of 2 mm. Based on the given geometric and material properties, the mass M and stiffness K of the bar with a cavity, that houses the ball, are calculated as 0.644 kg and 9.22 MN/m, respectively. The performance of the impact-damped bar is compared with that of an undamped (solid) boring bar to highlight the damping effect. For the solid bar, M and K are estimated as 0.668 kg and 9.26 MN/m, respectively. The damper ball is assumed to be made of carbide, weighing 26 grams, and two gap sizes of 0.1 mm and 1.0 mm are considered for the analysis. The rolling friction coefficient is taken as 0.6 mm [15], and the COR for the carbide ball is taken as 0.5 in the analysis.

First, we present the results of the model-based analysis without accounting for rolling friction. In this case, Eqs. (1–2) are solved with F_{rf} omitted, and responses of both the bar and ball are evaluated. A representative case at a frequency ratio of 1 with a gap of 0.1 mm is shown in Fig. 2, showing the bar displacement, ball displacement, relative displacement, and relative velocity. As seen in Fig. 2(a–b), both the bar and ball displacements exhibit modulations and do not settle into a periodic steady-state response. The inset of Fig. 2(c) illustrates the relative displacement oscillating between ± 0.05 mm. When the ball strikes a sidewall, the relative displacement reaches half of the total clearance because the ball is assumed to be placed at the middle of the cavity in the model. At this instant, the relative velocity undergoes a reversal in direction, as depicted in the inset of Fig. 2(d). As evident from the inset of Fig. 2(c), both single and double impacts on a sidewall occur in combination. This irregular distribution of impacts induces modulations in the responses of both the bar and the ball.

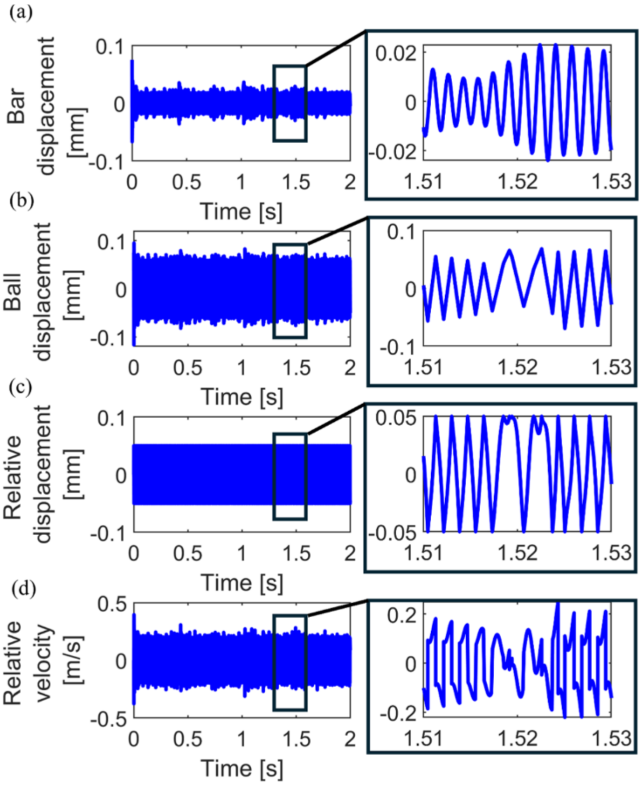

Fig. 2: Time history of impact-damped bar without friction for gap of 0.1 mm and frequency ratio of 1. (a) Bar displacement, (b) Ball displacement, (c) Relative displacement, and (d) Relative velocity.

Figure 2 presents the local behavior of the impact damper at resonance, illustrating the corresponding dynamics of the coupled system. To offer a broader perspective and better demonstrate the damping potential of the damper over a wide frequency range, Fig. 3 presents the root mean square (RMS) displacement of the boring bar without rolling friction. The results are shown for two gap sizes, 0.1 mm and 1 mm, comparing the performance of the damped and solid bars and highlighting the system's behavior near resonance. For each excitation frequency, the bar's displacement is computed, and the initial 20% of the total 2-second simulated time history is discarded while calculating the RMS value to remove transient effects.

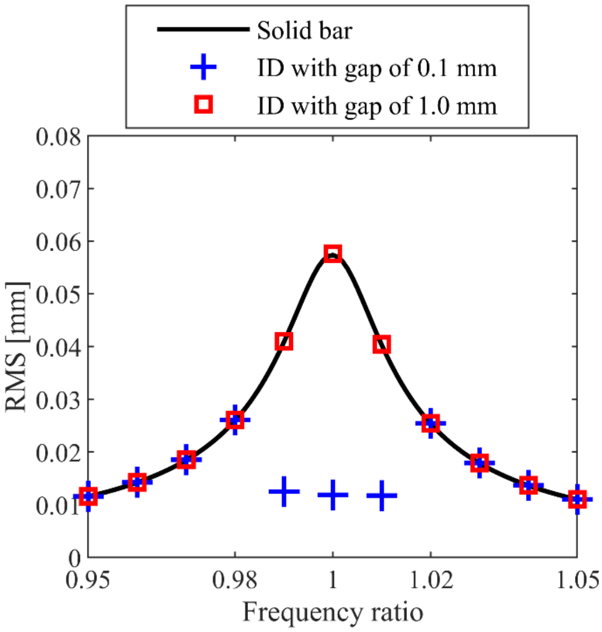

Fig. 3: RMS displacement response of impact-damped boring bar without friction.

As evident from Fig. 3, the RMS frequency response of the bar with the impact damper (ID) matches that of the solid bar across all discretized frequency ratios, indicating that a 1.0 mm gap is too large for the given external forcing to produce impacts. However, when the gap is reduced to 0.1 mm, near resonance at frequency ratios of 0.99, 1.00, and 1.01, the ball undergoes non-uniformly distributed impacts within each cycle of the bar's motion, as illustrated in a representative case in Fig. 2, thereby leading to energy dissipation. Our analysis unveiled that for gaps of 0.25 mm or larger, the ball experiences no impacts, and the bar's response becomes equivalent to that of a solid bar.

Prior studies [1]–[3] have reported that a vibro-impact system undergoing two symmetric impacts per cycle is most effective for achieving maximum damping. In contrast, our results demonstrate that, in the frictionless case, even non-uniformly distributed impacts can substantially reduce the bar's response at resonance. As seen in Fig. 3, all three cases exhibit responses consistent with those in Fig. 2, demonstrating a significant reduction in the RMS displacement of the bar. Although the amplitude at resonance decreases by about 83% compared to the solid bar, the response remains strongly modulated and does not settle into a steady state. Since the dynamics of vibro-impact systems are sensitive to the ball's initial position, we evaluated the robustness of the bar's dynamics against different initial conditions by repeating the simulations with nonzero initial values of bar displacement and relative velocity. The results remained consistent, with negligible variation in RMS values. Similar behavior was observed for the other two frequency ratios, indicating that, despite yielding nonperiodic and unsteady responses, the dynamics are robust to changes in initial conditions, and the vibro-impact system remains effective in sufficiently suppressing the bar's vibrations.

Since the damper ball rolls over the cavity surface, and this interface cannot be perfectly frictionless, rolling friction is now taken into account. By solving Eqs. (1–2), the positions and velocities of both the bar and the ball are obtained. Fig. 4 presents a representative case at resonance for a gap of 1 mm with rolling friction. Unlike the frictionless case shown in Fig. 3, where the ball experienced no impacts for a 1 mm gap and the bar's response coincided with that of the solid bar, the inclusion of friction results in the ball undergoing nearly two symmetric impacts per cycle. The relative displacement in Fig. 4(c) attains half the gap at each impact in an almost symmetric manner, with a corresponding velocity reversal observed in Fig. 4(d). However, as illustrated in the inset of Fig. 4(a), the bar's response remains nonperiodic and does not converge to a steady state, consistent with the behavior observed in the frictionless model. Furthermore, although the ball's displacement in the inset of Fig. 4(b) appears visually periodic, it is not; subtle variations in magnitude become evident upon closer inspection over successive cycles.

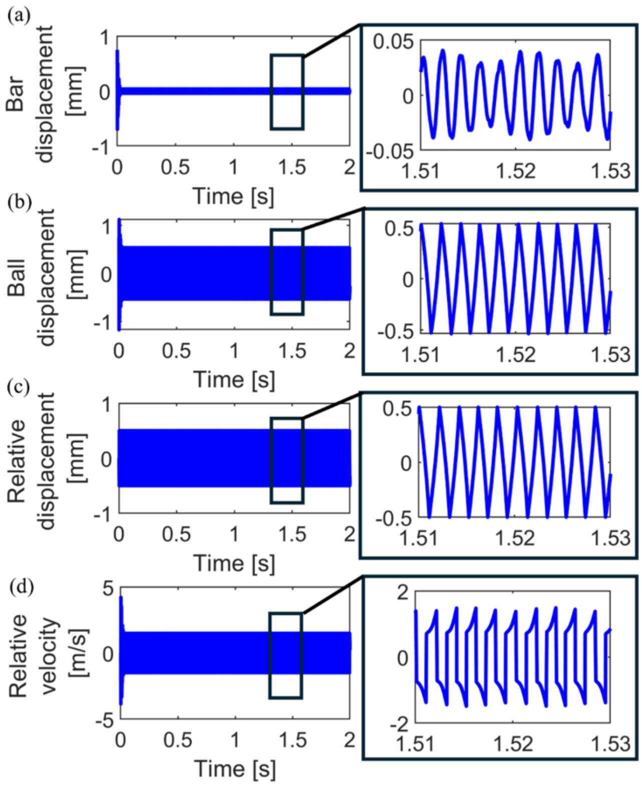

Fig. 4: Time history of impact-damped bar with friction for gap of 1 mm and frequency ratio of 1. (a) Bar displacement, (b) Ball displacement, (c) Relative displacement, and (d) Relative velocity.

Figure 4 provides a local view of the system's response at the resonance, illustrating the influence of rolling friction on the impact dynamics. To present a broader perspective, Fig. 5 shows the RMS displacement frequency responses of the solid and impact-damped bars for the friction case, similar to the analysis shown in Fig. 3. Unlike the frictionless case, where a 0.1 mm gap allowed impacts only at three excitation frequencies near resonance, and at other excitation frequencies, the bar's response overlapped with that of the solid bar, in the friction case the ball experienced impacts across the entire frequency range, and shows a leftward shift in the response and a peak value higher than that of the solid bar. In the presence of friction, part of the bar's energy is dissipated through dry friction. As a result, under the same amplitude of external forcing of 15 N, the ball impacts the bar not only for a gap of 0.1 mm but also for larger gaps. When the gap increases to 1.0 mm, the response becomes nearly independent of excitation frequency, consistent with the observations in [2]. For the 1 mm gap, the RMS response remains unchanged across frequency ratios; however, the time histories reveal that none of the cases reach a steady state, as illustrated in the representative case shown in Fig. 4. We also examined the sensitivity of the response to initial conditions and found almost no changes.

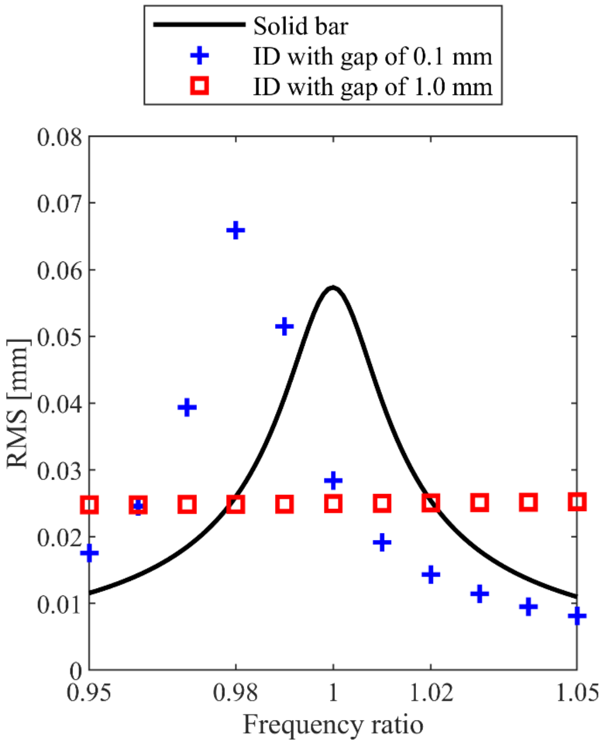

Fig. 5: RMS displacement response of impact-damped boring bar with friction.

Furthermore, for the 0.1 mm gap, each sidewall experiences only one impact, with the impact frequency varying with the frequency ratio. The impacts occur at non-uniform time intervals, and although the bar responses remain nonperiodic, they do not exhibit the pronounced modulations observed in the frictionless case (see Fig. 2(a)). Near resonance, both gaps yield nearly the same damping level, corresponding to an approximate 56% reduction in RMS displacement compared with the solid bar. Above resonance, the 0.1 mm gap provides superior damping, whereas below resonance, up to a frequency ratio of 0.98, the 1 mm gap is more effective. For frequency ratios below 0.98, however, the vibro-impact system yields a response worse than that of the solid bar.

Our analysis shows that with friction, impacts occur even at larger gaps and are neither entirely random nor absent over multiple cycles of the bar's motion, unlike in the frictionless case. As a result, the displacements of the bar and ball do not display noticeable modulations. The ball tends to undergo nearly two impacts per cycle, although its frequency varies with the gap. When the response approaches periodicity and the ball experiences close to two symmetric impacts per cycle, the impact damper provides sufficient damping. However, even under the most favorable gap in the frictional case, the damping performance remains inferior to that of the frictionless case, where nonuniformly distributed impacts yield larger vibration suppression.

IV. Conclusion

This paper presented a model-based analysis of a vibro-impact system integrated into a boring bar for vibration-free machining. A lumped-parameter model of the bar with rolling friction between the impacting ball and the bar was used, and dynamic analysis under harmonic forcing acting at the free end was performed with varying excitation frequencies to evaluate the damping potential near resonance.

Results revealed that, for a fixed excitation magnitude, the frictionless vibro-impact system experiences impacts only when the gap is as small as 0.1 mm and the bar is excited near resonance. In contrast, when friction is included, the damper ball experiences impacts even for larger gaps, such as 1 mm. At resonance, the frictionless case showed an 83% reduction in the bar's response at a 0.1 mm gap with the ball undergoing non-uniform impacts, whereas with friction, the response at a 1 mm gap was reduced by 56% with the ball undergoing nearly two impacts per cycle. These results indicate that neglecting friction in the vibro-impact model can lead to an overestimation of damping compared to real systems, where friction plays a critical role. This study addresses a key gap by explicitly accounting for rolling friction in vibro-impact damped boring bars, but further work, including experimental validation and a continuous beam model for optimal damper placement, is needed.

References

[1] S. F. Masri, "On the Stability of the Impact Damper," *J. Appl. Mech.*, vol. 33, no. 3, pp. 586–592, 1966, doi: https://doi.org/10.1115/1.3625125.

[2] S. F. Masri, "General Motion of Impact Dampers," *J. Acoust. Soc. Am.*, vol. 47, no. 1B, pp. 229–237, 1970, doi: 10.1121/1.1911470.

[3] M. M. Sadek, "The Behaviour of the Impact Damper," *Proc. Inst. Mech. Eng.*, vol. 180, no. 1, pp. 895–906, 1965, doi: 10.1243/pime_proc_1965_180_058_02.

[4] A. Patel, M. Law, and P. Wahi, "Vibration suppression of a slender boring bar by an impact damper," *Manuf. Technol. Today*, vol. 22, no. 4, pp. 14–19, 2023, doi: 10.58368/MTT.22.4.2023.14-19.

[5] A. Patel, M. Law, and P. Wahi, "Damping Chatter Vibrations of a Boring Bar by an Integrated Impact Damper BT - Proceedings of the 15th International Conference on Vibration Problems," 2024, pp. 305–314, doi: https://doi.org/10.1007/978-981-99-5922-8_28.

[6] Z. Iklodi, D. A. W. Barton, and Z. Dombovari, "Bi-stability induced by motion limiting constraints on boring bar tuned mass dampers," *J. Sound Vib.*, vol. 517, no. August 2021, p. 116538, 2022, doi: 10.1016/j.jsv.2021.116538.

[7] M. D. Thomas, W. A. Knight, and M. M. Sadek, "Impact Damper As a Method of Improving Cantilever Boring Bars.," *Am. Soc. Mech. Eng.*, no. 74-WA/DE-9, pp. 859–866, 1974, doi: doi: https://doi.org/10.1115/1.3438693

[8] E. Gourc, S. Seguy, G. Michon, A. Berlioz, and B. P. Mann, "Quenching chatter instability in turning process with a vibro-impact nonlinear energy sink," *J. Sound Vib.*, vol. 355, pp. 392–406, 2015, doi: 10.1016/j.jsv.2015.06.025.

[9] R. Chabrier, G. Chevallier, E. Foltête, and E. Sadoulet-Reboul, "Experimental investigations of a vibro-impact absorber attached to a continuous structure," *Mech. Syst. Signal Process.*, vol. 180, no. June, p. 109382, 2022, doi: 10.1016/j.ymssp.2022.109382.

[10] H. C. Yalamati, A. Patel, J. Bhoge, P. Wahi, and M. Law, "Experimental analysis of the dynamics of an impact damped boring bar," *Int. Conf. Precision, Micro, Meso Nano Eng.*,2024, in press.

[11] J. Bhoge, M. Kumar, H. Charan, A. Patel, and M. Law, "New vision-based evidence of the nature of vibro- impacts in an impact-damped boring bar," *Proc. 20th Int. Conf. Precis. Eng.*, 2024.

[12] S. Ema and E. Marui, "Suppression of chatter vibration of boring tools using impact dampers," *Int. J. Mach. Tools Manuf.*, vol. 40, no. 8, pp. 1141–1156, 2000, doi: 10.1016/S0890-6955(99)00119-4.

[13] C. C. Cheng and J. Y. Wang, "Free vibration analysis of a resilient impact damper," *Int. J. Mech. Sci.*, vol. 45, no. 4, pp. 589–604, 2003,

doi: 10.1016/S0020-7403(03)00116-4.

[14] R. Jankowski, "Non-linear viscoelastic modelling of earthquake-induced structural pounding," *Earthq. Eng. Struct. Dyn.*, vol. 34, no. 6, pp. 595–611, 2005, doi: 10.1002/eqe.434.

[15] Y. Wei-ming, W. Bao-shun, and H. Hao-xiang, "Research of mechanical model of particle damper with friction effect and its experimental verification," *J. Sound Vib.*, vol. 460, p. 114898, 2019, doi: 10.1016/j.jsv.2019.114898.

[16] P. Hagedorn A. DasGupta, *Vibrations and waves in continuous mechanical systems*. England: John Wiley & Sons, Ltd, 2007.